Published in final edited form as:
NMR Biomed. 2009 January ; 22(1): 65–76. doi:10.1002/nbm.1217.

Metabolite quantification and high-field MRS in breast cancer

Ihab S. Haddadin, **Adeka McIntosh**, **Sina Meisamy**, **Curt Corum**, **Angela L. Styczynski Snyder**, **Nathaniel J. Powell**, **Michael T. Nelson**, **Douglas Yee**, **Michael Garwood**, and **Patrick J. Bolan***
Center for Magnetic Resonance Research, Department of Radiology, University of Minnesota Cancer Center, University of Minnesota Medical School, Minneapolis, MN, USA

Abstract

In vivo ^{1}H MRS is rapidly developing as a clinical tool for diagnosing and characterizing breast cancers. Many *in vivo* and *in vitro* experiments have demonstrated that alterations in concentrations of choline-containing metabolites are associated with malignant transformation. In recent years, considerable efforts have been made to evaluate the role of ^{1}H MRS measurements of total choline-containing compounds in the management of patients with breast cancer. Current technological developments, including the use of high-field MR scanners and quantitative spectroscopic analysis methods, promise to increase the sensitivity and accuracy of breast MRS. This article reviews the literature describing *in vivo* MRS in breast cancer, with an emphasis on the development of high-field MR scanning and quantitative methods. Potential applications of these technologies for diagnosing suspicious lesions and monitoring response to chemotherapy are discussed.

Keywords

breast; cancer; MRS; quantification; choline; high-field MR

INTRODUCTION

Breast cancer is a very common disease, affecting one in eight American women in their lifetimes and causing more than 40 000 deaths each year (1). MRI is increasingly being used for various imaging needs in managing breast cancer, such as local staging and screening high-risk patients. Over the past 10 years, researchers have explored the use of ^{1}H MRS for characterizing breast cancers, and have shown that it can be used to improve diagnostic accuracy and monitor response to therapy. It appears that MRS may have a clinical role as a complementary measurement to augment a breast MRI examination, providing improved accuracy to the overall MR examination.

In vivo breast MR spectra may exhibit a resonance at ~3.2 ppm that is known to be associated with malignancy. Several chemical resonances contribute to this observed peak, including phosphocholine (3.21 ppm), glycerophosphocholine (3.22 ppm), and free choline (3.19 ppm), as well as contributions from taurine (3.25 ppm), *myo*-inositol (3.27 ppm), phosphoethanolamine (3.23 ppm), and glucose (3.24 ppm) (2) [with shift assignments from ref. (3)]. These contributions can be separated in *ex vivo* MR studies, but *in vivo*, the resonances are broader and appear as a single peak, referred to as total choline-containing compounds (tCho).

*Correspondence to: P. J. Bolan, Center for Magnetic Resonance Research, 2021 Sixth Street SE, Minneapolis, MN 55455, USA., E-mail: bolan@cmrr.umn.edu.

Ex vivo and *in vitro* studies have shown that it is primarily intracellular phosphocholine that is increased in malignancies and that this aberrant increase in concentration parallels various stages of tumorigenesis, with higher-grade breast lesions associated with higher phosphocholine concentrations (4,5). The cause of this aberrant increase is still being investigated. Mechanisms postulated thus far include increased activity of choline kinase (6, 7), increased phospholipase C expression (7), upregulated choline transporter concentrations (8), and increased activation of phospholipase A_2 (9) and phospholipase D (10). The elevated tCho signal that can be observed in many *in vivo* cancers can be attributed to both the increase in intracellular phosphocholine concentration and the increased density of cancer cells in the lesion.

The aim of most breast ^{1}H MRS studies reported to date has been to determine if the detectability of a tCho resonance in a breast lesion is indicative of malignancy. This use of tCho as a cancer biomarker has been successfully demonstrated at many sites using 1.5 T MR scanners and a variety of acquisition and analytical techniques. The working assumption for these studies is that higher tCho concentrations in malignancies make it easier to detect a tCho resonance. Quantitative breast MRS methods aim to measure the actual concentration of tCho ([tCho]), thus measuring the biological condition more directly without confounding experimental conditions – such as variable measurement sensitivity – that affect signal detectability. A quantitative estimate of [tCho] is also necessary to compare measurements from experiments with potentially different sensitivities, as in performing longitudinal studies with shrinking lesions or when comparing results across different sites or MR scanners. Furthermore, quantitative methods extract more information from a given study and enable more sophisticated statistical analyses.

Although MRS quantification is feasible and valuable on 1.5 T scanners, the accuracy and precision of quantitative MRS can greatly increase with higher field strengths. The approximately linear increase in sensitivity (11,12), along with greater spectral resolution (13), can improve detectability of tCho and other metabolites, decrease measurement errors, and enable the study of smaller lesions. The synergistic combination of high-field MR and quantitative methods has potential for greatly improving the clinical utility and availability of breast MRS. Nevertheless, whereas there have been several publications describing breast MRS at 4 T (14–18), there have only been a few reports describing initial experiences at 3 T (19,20) and 7 T (21).

The aim of this article is to review and discuss the techniques and applications of quantitative and high-field breast MRS. We hope that this work will improve understanding of quantitative MRS methods and encourage greater implementation of breast MRS studies. We also intend to describe the benefits and limitations of high-field breast MRS, to guide interpretation of future developments at 3 T and higher field strengths.

ACQUISITION TECHNIQUES

The quality of MRS measurements depends primarily on MR sensitivity, spectral resolution, localization performance, and the presence of experimental artifacts. The sensitivity of the measurement, often described as the signal-to-noise ratio (SNR), determines what signals can be detected and how precisely they can be quantified. Sensitivity increases linearly with voxel volume, approximately linearly with increasing B_0 field strength, and with the square root of the number of averages acquired. The signal reception performance of various breast coil designs is also highly variable, as coil comparisons have shown large variations in sensitivity with both custom-made and commercial breast coil designs (22–24). Increased spectral resolution also improves the ability to detect, quantify, and distinguish different resonances

(13). Spectral resolution can be increased by using higher B_0 field strengths and by optimizing B_0 shimming methods to improve field homogeneity over a given region of interest (ROI).

Localization quality is critical to ensure that the MRS signal comes from the correct ROI. The vast majority of breast MRS studies have been performed using single-voxel spectroscopy (SVS), with localization techniques such as PRESS (25,26), STEAM (27), and LASER (28). This approach is generally well suited to studying a single breast lesion. These techniques provide good localization and enable the operator to adjust the acquisition parameters (such as power, B_0 shim, water suppression, etc.) for a focused ROI. However, SVS techniques do not give any information regarding the spatial variation of spectroscopic signals. This information can be obtained by using spectroscopic imaging (SI). Several papers and numerous recent abstracts have shown that it is feasible to perform SI in breast on clinical MR systems (29–32). SI can be beneficial for breast cancers because tumors are often inhomogeneous, and also because properly selecting a single-voxel ROI within a tumor requires experience and skill. For these reasons, SI can simplify acquisition planning and provide more information about tumor structure. Unfortunately, SI is more technically challenging than SVS, because B_0 shimming, fat suppression, precise localization, and quantification are all substantially more difficult. The majority of the work described in this review used SVS.

High-quality 3D imaging is necessary to accurately identify the target lesion and plan the ROI for MRS acquisition. Typical SVS protocols use a dynamic contrast-enhanced (DCE) MRI series before MRS planning. The images are then processed and analyzed, and a voxel is positioned and sized on the lesion of interest in all three dimensions. This planning stage must be short to minimize delays and potential subject motion, and thus requires some expertise in breast MR image analysis. The size and position of the voxel is planned to maximize coverage of the lesion, while minimizing inclusion of adjacent fibroglandular or adipose tissues. This can be a difficult compromise; increasing the voxel size improves SNR but can make the measurement less specific and can potentially introduce artifacts from adipose tissues. Voxel planning in longitudinal studies such as monitoring treatment response is further complicated by variable positioning of the breast in the coil as well as changes in tumor size and conformation. In addition, the voxel placement should avoid obvious cysts (as these have highly variable metabolite concentrations) and signal voids from necrotic regions or radiographic markers, as these can degrade the quality of B_0 shimming (Fig. 1).

Water and lipid suppression

Breast spectra can exhibit both large water (4.7 ppm) and lipid (1.3 ppm) resonances depending on the composition of tissue within the voxel. Spectra from adipose tissue primarily show lipid resonances and a small water resonance (Fig. 2b), whereas spectra from normal fibroglandular tissues generally show a large water resonance and lipid resonances of varying amplitude. An MRS voxel placed entirely within a non-necrotic tumor will show mostly water along with some substantially smaller lipid resonances. Most voxels placed in breast cancers include some fibroglandular and adipose tissues, and also potentially lipid-rich necrotic regions. This leads to wide variations in the relative amounts of water and lipid in breast cancer spectra.

Several strategies have been used to deal with the potentially large 1.3 ppm lipid resonance in breast spectra. One approach is to perform water suppression and no lipid suppression. The large lipid resonance often observed can distort the baseline and lead to sideband artifacts, as shown in Fig. 2a. These sideband artifacts are due to oscillations of the B_0 field during the beginning of the acquisition, and have been attributed to mechanical oscillations of the gradient coils (33). These artifacts can be removed by using only the modulus of the complex spectra (34), or by experimentally resolving the sidebands using a two-dimensional *J*-resolved technique (35). A practical implementation of the two-dimensional *J*-resolved approach is to

average spectra acquired at different *TE*s, thus using destructive interference to cancel out the phase-sensitive sidebands while preserving non-coupled resonances. This technique, called *TE* averaging, has been shown to reduce artifacts in breast spectra (14). A variation on this approach is to acquire breast spectra at several distinct *TE*s to verify that the metabolite is observed consistently at each *TE* (36–38).

A final alternative is to use lipid suppression to reduce or eliminate the large 1.3 ppm lipid resonance (29,39,40). This approach does eliminate the sideband artifact problem, but intra-voxel lipids can still affect a tCho measurement. There is a 3.2 ppm lipid resonance detectable in pure adipose tissue, as shown in Fig. 2b. This leads to a partial volume problem which can artificially increase the estimate of tCho from a breast lesion when the water/fat ratio is less than 2 (15). None of the above methods can address this problem; the only available solution is to adjust the voxel placement to reduce adipose tissues, which may not be feasible in certain heterogeneous or irregularly shaped lesions.

ANALYSIS TECHNIQUES

Frequency and phase post-processing

Breast spectral quality can be improved by post-processing techniques to correct frequency and phase variations before spectral analysis. In some studies, there may be some motion of the breast tissue due to respiration or subject motion, which can lead to phase variations between spectral averages (41). It is also now well known that even when motion of the breast tissue itself is negligible, respiratory-induced frequency variations that extend far from the moving thoracic organs can cause frequency shifts between consecutive spectra (16,42). The magnitude of these frequency variations scales linearly with the magnetic field and so is constant on a ppm scale. The average peak-to-peak frequency variation in breast spectra has been reported to be ~0.14 ppm at both 4 T and 7 T (16,21). Without correction, these effects can broaden spectral linewidths and reduce quantification accuracy. They are, however, easily corrected retrospectively using frequency and phase corrections before averaging (39,41–44), although this technique is not yet commonly implemented on commercial MR systems.

Detecting tCho

A variety of methods have been used for analyzing the tCho resonance in breast spectra. The most widely used approach is to have an experienced observer make a subjective determination of whether or not a resonance is present at 3.2 ppm. An alternative and more objective method is to measure the SNR of the region around the suspected tCho resonance, and if it is greater than some pre-defined threshold (e.g. SNR $\geq$2), then the spectrum is considered to be positive for tCho. Typically, SNR is measured using the peak intensity (height, not area) and measuring the noise intensity in an off-resonance region in the spectrum. Both of those methods simply determine if a resonance is detectable, which has been generally interpreted as an indicator of malignancy. The underlying assumption of this interpretation is that, if there are high concentrations of choline-containing compounds within the voxel, resulting from either high intracellular phosphocholine concentrations and/or high cellular density, then it is more likely that a tCho resonance will be detected.

The use of tCho detectability as a surrogate for increased phosphocholine is problematic because it assumes that the sensitivity for detecting tCho does not change between comparable measurements. However, numerous factors can substantially affect the detectability of tCho independently of the underlying biology. The sensitivity of the measurement – and thus the detectability of tCho – increases linearly with voxel size and approximately linearly with increasing field strength (11,12). Sensitivity is also heavily dependent on the breast coil signal reception performance, which varies between different coil designs, changes between subjects

due to different coil loading, and depends on the spatial position of the voxel relative to the coil elements. The tCho signal intensity also varies with the number of signal averages, *TE*, *TR*, T_1 and T_2 relaxation rates, and the quality of B_0 shimming. Finally, the adipose tissue partial volume also affects tCho sensitivity, as low water/fat ratios indicate that the aqueous compartment (which contains the water-soluble choline metabolites of interest) is substantially smaller than the voxel size. When detectability is used as a malignancy biomarker, it is necessary to control all of these factors to compare data between different subjects.

Quantifying tCho

Rather than simply detecting a tCho resonance, quantitative methods aim to produce a numerical metric that is, at minimum, proportional to the concentration of all choline-containing compounds in a voxel. If all the factors discussed above that affect sensitivity are controlled, then the tCho SNR may be a suitable quantitative metric. Methods that strive for absolute quantification intend to produce a metric that estimates the actual concentration of all the choline-containing compounds in a voxel. The term absolute should not be interpreted as 'perfect' or 'correct', as this would require external validation that is not feasible in human subjects; rather it reflects that the metric is independent of the means of measurement and is therefore reported in real-world units. This is done by correcting for all known and measurable sources of scaling and bias in the experimental data. The area under the 3.2 ppm tCho resonance in the frequency domain is proportional to the number of ^{1}H atoms resonating at that frequency, but it is also scaled by the MR scanner's amplification and all the sensitivity-related factors discussed in the previous section. Absolute quantification methods take all of these factors into account and correct for them if necessary.

Quantitative spectral analysis consists of two steps: (1) estimating the signal amplitudes of the various metabolites, and (2) converting the signal amplitude into a concentration using a referencing strategy. The tCho signal amplitude is generally estimated by fitting the spectral data to a model and evaluating the goodness of fit. A variety of fitting tools have been used for *in vivo* breast MRS: Baik *et al.* (45) and Klomp *et al.* (46) used the jMRUI package (47); Tan *et al.* (48) used the commercial LC Model (49); our group (15) used a home-built implementation of TDFDFit (50); Bakken *et al.* (51) used the peak integration tools provided by the MR scanner manufacturer. Most of these tools use Cramér–Rao bounds as a surrogate of the parameter estimation error. This error estimation is critical, as it is used for setting detection thresholds and evaluating the quality of the data. Cramér–Rao bounds are widely used in MRS analysis, because they account for both SNR and the appropriateness of the model (52). The Cramér–Rao theory, however, has a number of limitations and its performance deteriorates at low SNR, which is common in breast MRS. Other methods of estimating error, such as non-parametric methods (53,54) or confidence intervals (55), may be more suitable for setting detection criteria and merit further investigation.

Two referencing strategies have been used for converting measured signal amplitudes into concentrations. The first method is external referencing, in which the *in vivo* measurement is compared with a measurement from an external phantom of known concentration. Roebuck *et al.* (56) was the first to use this approach in breast MRS, by measuring *in vivo* tCho peak SNR, comparing this value with a separate phantom measurement, and correcting for voxel size and spectral linewidth. They did not correct for coil loading, coil spatial sensitivity, and tCho T_1 and T_2 relaxation, as they estimated that these effects would be negligible. They reported a measurable tCho resonance in 7/10 cancers, with concentrations from 0.7 to 2.1 mM in voxels ranging from 1.0 to 1.8 mL, and one benign tubular adenoma with a concentration of 5.8 mM in a 9.8 mL voxel. Bakken *et al.* (51) also investigated the external referencing method and evaluated it on a single patient. In their method, a calibration phantom was positioned in the coil during the patient study. A spectrum was acquired from the patient, and

then a reference measurement was made in the calibration phantom while the patient remained in the same position. This eliminates variations in coil loading between the *in vivo* and reference measurements. They also corrected for number of averages, T_1 and T_2 relaxation, and, like Roebuck *et al*., determined that the spatial variation of coil sensitivity was negligible. In the one patient measured, they determined [tCho] = 2.0 mM in a 4 mL voxel.

The second referencing strategy proposed for breast MRS is to use the water peak from a non-suppressed spectrum from the same voxel as an internal reference. This approach is commonly used in brain MRS and was demonstrated in breast MRS by our group (15) on a 4 T research scanner, and later used by several other groups on clinical 1.5 T machines (45,46,48). The tCho concentration is calculated by comparing the tCho and water signal intensities and correcting for the differences in relaxation, signal averaging, and system gain. This ratio can then be converted into a molal unit (mmol tCho per kg water), or, by assuming a water density and aqueous fraction, a molar unit (mmol per liter, mM). The units are comparable – assuming a water density of 1 kg/L and 100% aqueous fraction, 1 mmol/kg is equivalent to 1 mM. An advantage of the internal referencing method is that it is relatively insensitive to the inclusion of adipose tissue in the voxel. The water and 3.2 ppm resonances from adipose tissue are small compared with those from fibroglandular tissue and most lesions. Therefore, including a small amount of adipose tissue within the SVS voxel will reduce both the water and tCho resonance amplitudes equally and not substantially affect the tCho/water ratio, whereas an externally referenced tCho measurement would be reduced. Our work at 4 T showed that adipose partial volumes of less than ~33% did not bias the internally referenced tCho concentration (15). The internal reference approach produces tCho concentration estimates that are similar to but somewhat higher than the external approach. We originally reported concentrations of 0.5–8.6 mmol/kg (15); Klomp *et al*. (46) reported 0.5–10.0 mmol/kg; Tan *et al*. (48) reported 2.9–11.9 mM; Baik *et al*. (45) originally reported relatively high values of 0.8–21.2 mmol/kg, and in a later abstract reported values more consistent with the other studies, 0.7–11.5 mmol/kg (57).

Compared with the external referencing strategy, the internal referencing technique is simpler and automatically corrects for several important experimental factors, including coil transmit efficiency, coil receive sensitivity, voxel size, and partial voluming with adipose tissue. However, the internal approach is sensitive to changes in the T_2 and NMR visibility of water that do not affect the externally referenced techniques. It is known that breast water content and T_2 varies under normal physiological conditions (58) and during chemotherapy (59). The possibility of confounding internally referenced tCho measurements with varying water content can be minimized by using the shortest possible *TE* for the water reference, accounting for water T_2 variations in the quantification method, and by performing externally referenced quantification of the water content as a control.

Peak ratios

These quantitative methods using sophisticated spectral fitting and referencing strategies are designed to maximize the information available in a MRS measurement, but their complexity has limited their widespread applicability. A simpler approach is to use peak ratios, as is commonly done in brain and prostate MRS. Using a tCho/water ratio (i.e. normalizing the tCho peak intensity by the intensity of the unsuppressed water peak) gives many of the advantages of the internally referenced quantitative method with greatly reduced complexity. At higher field strengths at which other metabolites may be routinely detectable, the tCho resonance could be normalized by the creatine or taurine resonances that are present in healthy fibroglandular tissues.

Some of the earliest breast MRS work proposed using the water/fat ratio as a marker of cancer, with the observation that tumors have higher water/fat ratios than normal tissues and that this information can be used to measure response to therapy (60–62). Subsequent studies have

suggested that this ratio is not specific, as it can reflect adipose tissue partial volume contamination and is sensitive to voxel placement (15,56,63). Recent work showing that the water/fat changes during therapy could predict anatomical response attributed the majority of the water/fat changes to changes in water T_2, rather than changes in the tumor lipid content (59).

Confounding effects: relaxation and contrast agents

Both internal and external referencing strategies require some correction or at least consideration of the T_1 and T_2 relaxation rates of the tCho, and potentially water and lipid as well. Table 1 summarizes the reported relaxation rate constants for water, 1.3 ppm lipid, and tCho at various field strengths. The values for water are most consistent, showing decreasing T_2 and increasing T_1 with higher field strengths (note that the post-Gd water T_1 measurements depend on lesion vascularity and contrast dynamics and should not be used). Measurements of the tCho relaxation times are difficult because of the low SNR, and are therefore quite variable. For most studies, an average tCho T_1 and T_2 must be assumed. It is feasible, however, to measure water T_1 and T_2 for each voxel studied, and remove a potential source of physiological variation. Manton *et al*. (59) recently showed that spectroscopically measured water T_2 could be used as both a predictive and monitoring biomarker in breast cancer chemotherapy. They reported that tumors that eventually responded had a longer T_2 before therapy than those that would not respond to therapy ($p = 0.03$). In addition, the decrease in T_2 during therapy predicted response with 69% accuracy and 100% specificity.

T_2 measurements can also be important in the diagnostic setting. Our group reported a diagnostic study in 81 patients using quantitative breast MRS along with spectroscopic T_2 measurements in each voxel (64). The water T_2 of benign lesions ($n = 37$, mean 65.4 ms) was longer ($p = 0.001$) than the T_2 in malignant lesions ($n = 44$, mean 55.4 ms). A tCho resonance could be quantified in 44 of these patients. Figure 3 shows the calculated [tCho] using a fixed T_2 value (60 ms) for the entire dataset (fixed T_2), compared with the [tCho] calculated using the T_2 value measured in each voxel (T_2 corrected). The unexpected finding was that the T_2 corrected data were less accurate in separating benign from malignant lesions than those using a fixed T_2. This indicates that the fixed T_2 [tCho] measurement is confounded by a water T_2 effect, albeit in this case the effect was beneficial. It is clear from both this study and that by Manton *et al*. (59) that the water T_2 should be measured in each voxel. The optimal way to combine the [tCho] and water T_2 data, however, is not yet known. It may be feasible to use multi-parametric analysis techniques, such as ISODATA (65), logistic regression analysis (59), or statistical classification strategies (66), to extract the maximum information from these single-voxel measurements.

Gd-based contrast agents can also affect relaxation rates, as well as increase spectral linewidths due to magnetic susceptibility changes. Studies of Gd and brain MRS have variously reported decreases in tCho area (67), peak broadening only with no loss of area (68), and no detectable effects (69,70). These studies were all performed on brain tumors. Although many breast MRS papers have expressed concern about the effects of Gd, there have only been two reports describing the effect of Gd on breast MRS. The first was a small study from our group, in which six breast tumors were measured with MRS before and ~10 min after a 1 mmol/kg bolus of gadopentetate dimeglumine (71). We found that the post-contrast spectra had water peaks that were 20% broader and tCho resonances that had 10% less area compared with pre-contrast spectra. A more recent and extensive report described MRS measurements at 1.5 T both before and after contrast (a fixed 20 mL bolus of gadodiamide) in 22 examinations of 15 subjects (72). This study found that Gd produced an increase in linewidth (~17%) and a decrease in peak area (~15%) of the tCho resonance. In all but two of the 22 examinations, however, the shim currents were not adjusted for the post-contrast measurements, as would be typically done

in a normal MRS examination. Both of these studies demonstrate that contrast agents can affect MRS measurements; however, it is not yet clear if the effects of contrast agents would significantly bias MRS measurements performed in a typical MRS scan.

APPLICATION: DIAGNOSING SUSPECT LESIONS

The most widely investigated application of breast MRS is for diagnosing suspicious lesions. There have been a large number of studies performed at 1.5 T showing that MRS can be clinically useful in this context. The general observation is that, when SVS is used with standard pulse sequences and commercially available breast coils, a tCho resonance can be detected in malignant lesions and not in benign lesions. There have been nine publications that support this finding, with sensitivities of 70–100% and specificities of 67–100% (36–38,56,73–76, 85). A retrospective study combining the results from five of these studies showed a net sensitivity and specificity of 83% and 85%, respectively (78). The consistency of these findings across numerous institutions with different MR systems and measurement techniques demonstrates that breast MRS is clinically practical and useful in this diagnostic context.

These studies have all used the detection of tCho, determined by either visual inspection or a threshold SNR level, to determine if a lesion is cancerous. Because of the success of this relatively simple procedure, there has been no widespread effort to move to more complicated quantitative methods. However, as discussed in the previous section, the use of detectability of tCho as a cancer biomarker assumes a constant sensitivity across all measurements. Variations in pulse sequences, MR systems, breast coils, and voxel sizes could all potentially affect these findings. The use of variable voxel sizes, for example, is a potentially important confounding factor. The voxel volumes across these studies varied greatly, ranging from 0.7 to 27 mL, with a typical volume of ~2 mL. SNR (and therefore tCho detectability) varies linearly with the volume of the voxel, so it is easier to detect tCho in larger voxels. Indeed, the review by Katz-Brull *et al*. (78) pointed out that malignant lesions were generally larger than benign lesions, and the sensitivity of detecting tCho increased uniformly with increasing tumor size. In addition, a recent abstract comparing breast MRS at 1.5 T and 3 T reported that tCho could more consistently be detected in smaller cancers at 3 T than at 1.5 T (19). Therefore, both voxel size and the underlying tCho concentration contribute to the specificity of using tCho detectability as a marker of malignancy.

Quantitative methods could standardize diagnosis across multiple sites and take account of variable voxel sizes, coil sensitivity, and field strength. Figure 4 shows a summary of all the quantitative MRS measurements performed by our group in biopsy-confirmed breast lesions at 4 T, an update of the data presented in ref. (15). Clearly, tCho concentration is higher in cancers than in benign lesions or normal tissues, as expected. By performing a receiver operating curve (ROC) analysis, an optimal cutoff can be selected for separating benign from malignant lesions. A cutoff of 1.45 mmol/kg gives a sensitivity of 73.2% and a specificity of 76.7% for distinguishing benign from malignant lesions. Note that the optimal cutoff value depends on the incidence of disease in the study population; the data in Fig. 4 are combined from several studies and do not represent a typical high-risk screening population.

The data in Fig. 4 show that there are many cancers with low [tCho], and a few benign lesions with raised [tCho]. Thus, quantitative MRS alone is not generally suitable for diagnosis and therefore should always be interpreted in a clinical context by incorporating information obtained from other imaging modalities and clinical data. For example, Jacobs *et al*. (79) described several subjects with negative or ambiguous findings on DCE MRI, who were found to have raised concentrations of tCho on the basis of MRS imaging. This suggested that combining MRI with MRS imaging may improve specificity over the use of either modality alone. A more quantitative example was presented by Huang *et al*. (76), who performed a

diagnostic study at 1.5 T that combined DCE MRI with SVS, by using a fixed SNR threshold to determine tCho detection. They found that DCE alone had 100% sensitivity and 62.5% specificity, but the addition of MRS improved the specificity to 87.5%. Our group performed a comparable study combining MRI with quantitative MRS measurements using blinded readers in an observer-performance study (18). With the use of an ROC analysis of the quantified tCho measurements, an optimal cutoff (1.03 mmol/kg) for distinguishing benign from malignant lesions was established. On the basis of that threshold, quantitative MRS alone gave 61% sensitivity and 83% specificity for diagnosis. Four radiologists, blinded to biopsy results and all clinical data, were then asked to evaluate MRI and MRS from all 55 subjects. We found that adding quantitative MRS to the MRI interpretation improved the sensitivity, specificity, accuracy, and interobserver agreement for all four radiologists. Overall it appears that there is some interdependence between the information provided by MRI and MRS. There is evidence that cancers with an aggressive phenotype, as determined by DCE MRI, also have greater amounts of tCho. Recent work has shown this relationship between MRS and qualitative DCE evaluation (80) and quantitative DCE parameters (30,81).

Choline in normal breast tissues

The observation that tCho detectability is associated with malignancy would suggest that tCho is not detectable in normal fibroglandular breast tissues at 1.5 T. Although several studies support this (36,63,77), Stanwell *et al*. (38) reported detecting a tCho resonance in 3/40 healthy, non-lactating volunteers at 1.5 T, with reasonable voxel volumes (3.1–6.1 mL). They further observed that the tCho peak in these cases was located at 3.28 ppm, rather than the 3.22 ppm position observed in cancers. They postulated that, in normal subjects, the tCho resonance may be attributable to taurine, *myo*-inositol, or possibly glycerophosphocholine, whereas in cancers it is primarily attributable to phosphocholine. Further studies are needed to confirm these findings. The lactating breast should be considered a special case, as several groups have reported both lactose and tCho resonance detectable in healthy lactating subjects at 1.5 T (36,38,73). Note also that tCho is commonly detectable in normal breast tissues at higher field strengths (Fig. 5).

APPLICATION: MONITORING TREATMENT RESPONSE

Breast MRS can also be used to evaluate response to therapy. The underlying principle is that increased tCho reflects the aberrant metabolism of the tumor cells, and any change in the cellular metabolism or viability will be reflected in the tCho concentrations before there is a detectable change in the tumor's vascular or morphological features. The first report of tCho changes in response to therapy in breast tumors was by Kvistad *et al.* (36), who observed that a subject undergoing neoadjuvant chemotherapy had a detectable Cho peak before treatment, but after treatment, the tCho resonance was no longer detectable. Jagannathan *et al*. (73) then performed a focused study and found that 10 patients who had a detectable tCho resonance before treatment all had either decreased or undetectable tCho resonance after three or six cycles of chemotherapy. These studies suggest that tCho could be used as a biomarker for monitoring therapy.

Our group then performed a pilot study using quantitative MRS in 13 patients undergoing doxorubicin-based neoadjuvant chemotherapy for locally advanced breast cancer (17). This study was performed on a research 4 T MR scanner, using custom-built single-breast coils (82). Patients were scanned once before treatment, 1 day after the first treatment, and again at the end of the chemotherapy regimen. Of the 13 patients who completed the protocol, the change in [tCho] between baseline and 1 day after the first dose of chemotherapy showed a significant positive correlation ($R = 0.79$, $p = 0.001$) with the change in lesion size measured at the end of four cycles of chemotherapy. The change in [tCho] at day 1 was significantly different between objective responders and non-responders ($p = 0.007$). These results suggest

that the decrease in [tCho] measured 1 day after the first dose of the drug could serve as an early indicator of clinical response to treatment for locally advanced breast cancer. These studies are ongoing. To date, we have complete data from 28 patients; 75% of objective responders showed a decrease in tCho 1 day after treatment, whereas 92% of non-responders showed no change or an increase in [tCho] 1 day after treatment (Fig. 6). Note also that the objective responders exhibited a higher pretreatment [tCho] ($p = 0.03$), suggesting that high concentrations of tCho at baseline might be a useful predictive biomarker for neoadjuvant chemotherapy.

More recently, several conference abstracts have described similar studies using clinical 1.5 T MR scanners, but with variable results. Tan *et al*. (48) performed a study of 18 patients receiving neoadjuvant chemotherapy using a 1.5 T scanner with a commercial breast coil, *TE*-averaged single-voxel MRS acquisition, and quantification with water as an internal reference. They observed no statistically significant difference between objective responders and non-responders in either baseline tCho concentrations or changes in tCho 1–8 days after the first cycle of therapy. Baik *et al*. (57) performed a similar study also at 1.5 T, performing single-voxel PRESS MRS and quantifying tCho using water as an internal reference. Seventeen patients with a measurable baseline tCho concentration were scanned after one or two cycles of therapy (follow-up 1) and again after completing the full course of treatment (follow-up 2). Six of the seven objective responders had decreased tCho at follow-up 1, and all seven had no detectable tCho at follow-up 2. The findings in the 10 non-responders were less specific, with approximately equal occurrences of increased and decreased tCho at both follow-ups. Overall, the responders showed a greater decrease in tCho at follow-up 1 than non-responders, but the difference between the groups was not significant. Both Tan *et al*. and Baik *et al*. reported no significant difference in pretreatment tCho concentrations between the objective responders and non-responders. In another recent study, Danishad *et al*. (83) used MRSI at 1.5 T and used the SNR of tCho as a metric of response. Note that, although this study did not use absolute quantification, the voxel size was kept constant during the study, which eliminates a major source of variation and allows comparison with the quantitative studies above. This study followed 11 patients at two post-therapy time points: after two and three cycles of therapy. The objective responders showed a greater decrease in tCho SNR (48%) than the non-responders (6%) after two cycles of therapy; after three cycles, the difference between the groups was greater (60% vs 17%, respectively).

Overall these findings are inconsistent with regard to the efficacy of MRS for monitoring response to therapy. There are methodological differences between the studies, most notably field strength, but also MR system manufacturers, coils, and sequences used. More importantly, perhaps, is the variation in protocol and timing of MR examinations. Whereas Meisamy *et al*. (17,18) confined post-treatment measurements to 1 day after the first treatment, Tan *et al*. reported measurements 1–8 days after the first treatment, Baik *et al*. after one to two cycles of therapy, and Danishad *et al*. after two cycles. This may partially explain the disparity between the findings. It may be that the utility of MRS is limited to the acute period of response (hours to a few days after therapy administration), during which anatomical changes are small and do not affect the sensitivity of the MRS measurement. Further work is required to determine the most effective post-therapy window.

All of these studies report that the ability to measure tCho decreases during the course of therapy, often resulting in no measurable tCho at the end of treatment. This is a major limitation of MRS measurements in responding tumors; as the lesion shrinks, it is more difficult to quantify tCho because there is less tumor in which to make measurements. This is an inherent problem with the relatively low sensitivity of MRS compared with MRI, which does limit the utility of MRS. Higher fields and more sensitive coils that enable tCho measurements in smaller voxels will reduce this problem but will not solve it.

Note also that performing MRS quantification over a course of treatment is particularly challenging because there are other physiological changes that can confound the tCho measurement. As lesion sizes change, variations in voxel placement and partial adipose volume are inevitable and must be accounted for. Successful therapy can also induce necrosis and increase intra-tumoral lipids. Several studies showing decreases in the water/fat ratio during successful therapy may be sensitive to both of these effects (59,61). For methods using water as an internal reference, it is necessary to account for the changing water T_2 relaxation rate constant, which also decreases in successful therapy (59).

HIGH-FIELD BREAST MRS

High fields can potentially improve the quality and utility of breast MRS because of increased sensitivity and spectral resolution. It is well established that the sensitivity of ^{1}H MRS increases approximately linearly with increasing field strength (11,12). This allows the practical voxel size to decrease proportionally when higher B_0 fields are used. The linear increase in spectral dispersion from higher fields is offset by an increase in magnetic susceptibility effects. The macroscopic susceptibility, however, can be minimized by B_0 shimming, leading to an overall increase in spectral resolution which allows different chemical resonances to be more easily resolved at higher fields (13). These improvements in both sensitivity and specificity contribute to the improved performance in quantitative MRS in the brain, where error estimates based on Cramér–Rao bounds have been shown to decrease more than linearly with increasing field strength (84).

One practical use of high field is to use the increased sensitivity to reduce the voxel size, enabling the study of smaller lesions. The feasibility of studying small voxels can be evaluated using a large set of quantified *in vivo* breast spectra acquired at 4 T, shown in Fig. 7. The data in this figure include 1359 spectra acquired from malignant, benign, and healthy breast tissue. Each data point indicates a spectroscopic measurement; blue dots indicate spectra with a detectable tCho resonance, and the red ‘X’ indicate spectra where no tCho resonance was detectable. The detectability of tCho is a function of voxel size, as seen in the lower plot. In the largest voxels, tCho is detectable with high regularity regardless of the actual concentration. In smaller voxels, only higher concentrations of tCho can be reliably quantified. For voxels 1–2 mL in size, the estimated errors for individual spectra are ≤ 1 mmol/kg in 55% of the cases. This represents a practical regime of operation. For voxels less than 1 mL in size, the errors increase dramatically and the measurements are less likely to be useful. Scaling back to 1.5 T, this would suggest that in voxels of 2.7–5.3 mL, a tCho of 1 mmol/kg or greater would be detectable in ~50% of the cases. Although there is great variation in coil sensitivity, voxel size, and tCho concentrations, these data are consistent with the literature describing breast MRS at 1.5 T.

The additional sensitivity and spectral resolution of higher fields may also allow detection of other metabolites in breast lesions. At 4 T, it is relatively common to detect distinct creatine and taurine resonances, although their SNR is substantially lower than that of tCho. Other metabolites in the 3.4–4 ppm region, including possibly alanine (3.78 ppm) and glycine (3.55 ppm), are also occasionally detectable, as shown in Fig. 8. At higher field strengths, it may be possible to use these signals for additional metabolic information or as markers of healthy tissue for normalization.

There are additional challenges associated with higher field strengths. B_0 shimming increases in difficulty, and B_1 inhomogeneities make coil designs more complicated (21). Relaxation rate constants also change: longer T_1 values may require longer *TR*s, shorter T_2 values will reduce signal intensities for a given *TE*, and both changes will increase the magnitude of relaxation corrections required for quantitative MRS. Experimental artifacts such as lipid

sidebands and respiratory-induced frequency shifts also increase at higher fields. In addition, at field strengths greater than 1.5 T, quantitative analyses will be required, as a tCho resonance can be detected routinely in normal subjects (Fig. 5). There are, however, techniques available for addressing all of these challenges, and the benefits of higher field strengths can be exploited to improve the value of breast MRS.

CONCLUSION

Proton spectroscopy can provide information that is clinically valuable for the management of patients with breast disease. Technological developments, such as quantitative MRS methods and high-field MR systems, have the potential to improve the accuracy and precision of breast MRS. Further advances are possible by increasing the sensitivity of breast coils and developing better B_0 shimming techniques. Future work on analytical methods will need to focus on improving methods for estimating measurement error, performing comparisons of various quantification strategies, and developing techniques for optimal combination of multi-parametric MR data (DCE MRI, [tCho], T_2, etc.). With the growing availability of 3 T systems and the increasing efforts by manufacturers to integrate and support body MRS techniques, it is feasible that the use of breast ^{1}H MRS for diagnosing lesions and monitoring response to therapy will become routine clinical practice. This will require a thorough knowledge of the capabilities and limitations of breast spectroscopy, established by reproducibility studies and multi-site validations.

Acknowledgements

Contract/grant sponsor: NIH; contract/grant number: CA120509, CA092004, RR008079 and RR00400.

Contract/grant sponsor: Tickle Family Land Grant Endowment in Breast Cancer Research.

Contract/grant sponsor: PHS Cancer Center Support; contract/grant number: P30 CA77398.

Contract/grant sponsor: Lillian Quist-Joyce Henline Chair in Biomedical Research.

We thank Tim Emory and Lenore Everson for numerous insightful discussions.

This work was supported by NIH grants CA120509, CA092004, RR008079 and RR00400, Tickle Family Land Grant Endowment in Breast Cancer Research, PHS Cancer Center Support Grant P30 CA77398, and the Lillian Quist-Joyce Henline Chair in Biomedical Research.

Abbreviations used

DCE
: dynamic contrast-enhanced

ROC
: receiver operating curve

ROI
: region of interest

SI
: spectroscopic imaging

SNR
: signal-to-noise ratio

SVS
: single-voxel spectroscopy

tCho

total choline-containing compounds

References

1. Ries, LAG.; Eisner, MP.; Kosary, CL.; Hankey, BF.; Miller, BA.; Clegg, L.; Mariotto, A.; Feuer, EJ.; Edwards, BK., editors. SEER Cancer Statistics Review 1975–2002. National Cancer Institute; Bethesda, MD: http://seer.cancer.gov/csr/1975_2002/, based on November 2004 SEER data submission, posted online 2005
2. Gribbestad IS, Sitter B, Lundgren S, Krane J, Axelson D. Metabolite composition in breast tumors examined by proton nuclear magnetic resonance spectroscopy. Anticancer Res 1999;19:1737–1746. [PubMed: 10470108]
3. Sitter B, Sonnewald U, Spraul M, Fjosne HE, Gribbestad IS. High-resolution magic angle spinning MRS of breast cancer tissue. NMR Biomed 2002;15(5):327–337. [PubMed: 12203224]
4. Aboagye EO, Bhujwalla ZM. Malignant transformation alters membrane choline phospholipid metabolism of human mammary epithelial cells. Cancer Res 1999;59(1):80–84. [PubMed: 9892190]
5. Podo F. Tumour phospholipid metabolism. NMR Biomed 1999;12 (7):413–439. [PubMed: 10654290]
6. Ramirez de Molina A, Rodriguez-Gonzalez A, Lacal JC. From Ras signalling to ChoK inhibitors: a further advance in anticancer drug design. Cancer Lett 2004;206(2):137–148. [PubMed: 15013519]
7. Glunde K, Jie C, Bhujwalla ZM. Molecular causes of the aberrant choline phospholipid metabolism in breast cancer. Cancer Res 2004;64(12):4270–4276. [PubMed: 15205341]
8. Eliyahu G, Kreizman T, Degani H. Phosphocholine as a biomarker of breast cancer: molecular and biochemical studies. Int J Cancer 2007;120(8):1721–1730. [PubMed: 17236204]
9. Guthridge CJ, Stampfer MR, Clark MA, Steiner MR. Phospholipases A2 in ras-transformed and immortalized human mammary epithelial cells. Cancer Lett 1994;86(1):11–21. [PubMed: 7954346]
10. Noh DY, Ahn SJ, Lee RA, Park IA, Kim JH, Suh PG, Ryu SH, Lee KH, Han JS. Overexpression of phospholipase D1 in human breast cancer tissues. Cancer Lett 2000;161(2):207–214. [PubMed: 11090971]
11. Hoult DI, Phil D. Sensitivity and power deposition in a high-field imaging experiment. J Magn Reson Imaging 2000;12(1):46–67. [PubMed: 10931564]
12. Vaughan JT, Garwood M, Collins CM, Liu W, DelaBarre L, Adriany G, Andersen P, Merkle H, Goebel R, Smith MB, Ugurbil K. 7 T vs. 4 T: RF power, homogeneity, and signal-to-noise comparison in head images. Magn Reson Med 2001;46(1):24–30. [PubMed: 11443707]
13. Gruetter R, Weisdorf SA, Rajanayagan V, Terpstra M, Merkle H, Truwit C, Garwood M, Nyberg SL, Ugurbil K. Resolution Improvements in *in vivo* ^{1}H NMR spectra with increased magnetic field strength. J Magn Reson 1998;135:260–264. [PubMed: 9799704]
14. Bolan PJ, DelaBarre L, Baker EH, Merkle H, Everson LI, Yee D, Garwood M. Eliminating spurious sidebands in ^{1}H MRS of breast lesions. Magn Reson Med 2002;48(2):215–222. [PubMed: 12210929]
15. Bolan PJ, Meisamy S, Baker EH, Lin J, Emory T, Nelson M, Everson LI, Yee D, Garwood M. *In vivo* quantification of choline compounds in the breast with ^{1}H MR spectroscopy. Magn Reson Med 2003;50(6):1134–1143. [PubMed: 14648561]
16. Bolan PJ, Henry PG, Baker EH, Meisamy S, Garwood M. Measurement and correction of respiration-induced B_0 variations in breast ^{1}H MRS at 4 Tesla. Magn Reson Med 2004;52(6):1239–1245. [PubMed: 15562472]
17. Meisamy S, Bolan PJ, Baker EH, Bliss RL, Gulbahce E, Everson LI, Nelson MT, Emory TH, Tuttle TM, Yee D, Garwood M. Neoadjuvant chemotherapy of locally advanced breast cancer: predicting response with *in vivo* (1)H MR spectroscopy: a pilot study at 4 T. Radiology 2004;233(2):424–431. [PubMed: 15516615]
18. Meisamy S, Bolan PJ, Baker EH, Pollema MG, Le CT, Kelcz F, Lechner MC, Luikens BA, Carlson RA, Brandt KR, Amrami KK, Nelson MT, Everson LI, Emory TH, Tuttle TM, Yee D, Garwood M. Adding *in vivo* quantitative ^{1}H MR spectroscopy to improve diagnostic accuracy of breast MR imaging: preliminary results of observer performance study at 4.0 T. Radiology 2005;236(2):465–475. [PubMed: 16040903]

19. Moy, L.; Hecht, E.; Do, R.; McGorty, KA.; Mercado, C.; Salibi, N. Can better breast MR spectroscopy (MRS) be obtained at 3T versus 1.5T?. Proceedings of the 92nd Annual Meeting RSNA; Chicago. 2006. p. 652
20. Do, R.; Moy, L.; Salibi, N.; Mercado, CL.; McGorty, K.; Kitazono, M.; Hecht, E. Can MRS improve our ability to distinguish between benign and malignant lesions?. Proceedings of the 14th Annual ISMRM; Seattle. 2006. p. 2876
21. Bolan, PJ.; Snyder, CJ.; DelaBarre, LJ.; Bolinger, L.; Garwood, M.; Vaughan, JT. Preliminary experience with breast ^{1}H MRS at 7 Tesla. Proceedings of the 14th Annual ISMRM; Seattle. 2006. p. 580
22. Konyer NB, Ramsay EA, Bronskill MJ, Plewes DB. Comparison of MR imaging breast coils. Radiology 2002;222(3):830–834. [PubMed: 11867809]
23. Zhai, X.; Kurpad, K.; Smith, M.; Mahay, D.; Harter, R.; Fain, S. Breast coil for real time MRI guided interventional device. Proceedings of the 15th Annual ISMRM; Berlin. 2007. p. 445
24. Giaquinto, RO.; McKenzie, C.; Sodickson, DK.; Grant, AK.; Murtagh, GE.; Furman, RL.; Swider, LJ.; Hardy, CJ.; Dumoulin, CL. A 28 channel bi-lateral breast array for accelerated MR imaging. Proceedings of the 14th Annual ISMRM; Seattle. 2006. p. 423
25. Bottomley PA. Selective volume method for performing localized NMR spectroscopy. US Patent 1984;4:480, 228.
26. Ordidge, RJ.; Bendall, MR.; Gordon, RE.; Connelly, A.; Govil, G.; Khetrapal, CL.; Saran, A. Magnetic Resonance in Biology and Medicine. McGraw-Hill; New Delhi: 1985. Volume selection for *in vivo* biological spectroscopy; p. 387-397.
27. Frahm J, Merboldt KD, Hanicke W. Localized proton spectroscopy using stimulated echoes. J Magn Reson 1987;72:502–508.
28. Garwood M, DelaBarre L. The return of the frequency sweep: designing adiabatic pulses for contemporary NMR. J Magn Reson 2001;153(2):155–177. [PubMed: 11740891]
29. Jacobs MA, Barker PB, Bottomley PA, Bhujwalla Z, Bluemke DA. Proton magnetic resonance spectroscopic imaging of human breast cancer: a preliminary study. J Magn Reson Imaging 2004;19 (1):68–75. [PubMed: 14696222]
30. Su MY, Baik HM, Yu HJ, Chen JH, Mehta RS, Nalcioglu O. Comparison of choline and pharmacokinetic parameters in breast cancer measured by MR spectroscopic imaging and dynamic contrast enhanced MRI. Technol Cancer Res Treat 2006;5(4):401–410. [PubMed: 16866570]
31. Hu, J.; Xuan, Y.; Latif, Z.; Soulen, RL. An improved ^{1}H magnetic resonance spectroscopic imaging technique for the human breast. Proceedings of the 13th Annual ISMRM; Miami. 2007. p. 134
32. Jacobs, MA.; Smith, M.; Khouri, N.; Bluemke, DA.; Barker, PB. Three-dimensional proton MR spectroscopic imaging of human breast lesions. Proceedings of the 14th Annual ISMRM; Seattle. 2006. p. 1795
33. Clayton DB, Elliott MA, Leigh JS, Lenkinski RE. ^{1}H spectroscopy without solvent suppression: characterization of signal modulations at short echo times. J Magn Reson 2001;153(2):203–209. [PubMed: 11740895]
34. Serrai H, Clayton DB, Senhadji L, Zuo C, Lenkinski RE. Localized proton spectroscopy without water suppression: removal of gradient induced frequency modulations by modulus signal selection. J Magn Reson 2002;154(1):53–59. [PubMed: 11820826]
35. Hurd RA, Gurr D, Sailasuta N. Proton spectroscopy without water suppression: the oversampled J-resolved experiment. Magn Reson Med 1998;40:343–347. [PubMed: 9727935]
36. Kvistad KA, Bakken IJ, Gribbestad IS, Ehrnholm B, Lundgren S, Fjosne HE, Haraldseth O. Characterization of neoplastic and normal human breast tissues with *in vivo* ^{1}H MR spectroscopy. J Magn Reson Imaging 1999;10:159–164. [PubMed: 10441019]
37. Yeung DKW, Cheung HS, Tse GMK. Human breast lesions: characterization with contrast-enhanced *in vivo* proton MR spectroscopy: initial results. Radiology 2001;220:40–46. [PubMed: 11425970]
38. Stanwell P, Gluch L, Clark D, Tomanek B, Baker L, Giuffre B, Lean C, Malycha P, Mountford C. Specificity of choline metabolites for *in vivo* diagnosis of breast cancer using ^{1}H MRS at 1.5 T. Eur Radiol 2005;15(5):1037–1043. [PubMed: 15351906]

39. Star-Lack JM, Adalsteinsson E, Gold GE, Ikeda DM, Spielman DM. Motion correction and lipid suppression for 1-H magnetic resonance spectroscopy. Magn Reson Med 2000;43:325–330. [PubMed: 10725872]
40. Baik HM, Su MY, Yu H, Mehta R, Nalcioglu O. Quantification of choline-containing compounds in malignant breast tumors by ^{1}H MR spectroscopy using water as an internal reference at 1.5 T. MAGMA 2006;19(2):96–104. [PubMed: 16779565]
41. Zhu G, Gheorghiu D, Allen PS. Motional degradation of metabolite signal strengths when using STEAM: a correction method. NMR Biomed 1992;5(4):209–211. [PubMed: 1449957]
42. Katz-Brull R, Lenkinski RE. Frame-by-frame PRESS ^{1}H-MRS of the brain at 3 T: the effects of physiological motion. Magn Reson Med 2004;51(1):184–187. [PubMed: 14705059]
43. Ziegler A, Decorps M. Signal-to-noise improvement in *in vivo* spin-echo spectroscopy in the presence of motion. J Magn Reson B 1993;102:26–34.
44. Helms G, Piringer A. Restoration of motion-related signal loss and line-shape deterioration of proton MR spectra using the residual water as intrinsic reference. Magn Reson Med 2001;46(2):395–400. [PubMed: 11477645]
45. Baik, HM.; Su, MY.; Yu, H.; Nalcioglu, O. Quantification of choline-containing compounds in malignant breast cancer by ^{1}H single-voxel MR spectroscopy at 1.5T. Proceedings of the 14th Annual ISMRM; Seattle. 2006. p. 582
46. Klomp, DW.; Veltman, J.; Boetes, C.; Barentsz, JO.; Heerschap, A. Robust quantification of choline compounds in the breast at 1.5T using prior knowledge and optimized detection methods. Proceedings of the 13th Annual ISMRM; Miami. 2005. p. 1854
47. van den Boogaart, A. A User's Guide to the Magnetic Resonance User Interface Software Package. Delft Technical University Press; Delft: 1997.
48. Tan, PC.; Lowry, M.; Manton, DJ.; Turnbull, LW. Evaluation of choline concentrations in malignant breast lesions in predicting response to neoadjuvant chemotherapy. Proceedings of the 14th Annual ISMRM; Seattle. 2006. p. 574
49. Provencher SW. Automatic quantitation of localized *in vivo* ^{1}H spectra with LCModel. NMR Biomed 2001;14(4):260–264. [PubMed: 11410943]
50. Slotboom J, Boesch C, Kreis R. Versatile frequency domain fitting using time domain models and prior knowledge. Magn Reson Med 1998;39(6):899–911. [PubMed: 9621913]
51. Bakken IJ, Gribbestad IS, Singstad TE, Kvistad KA. External standard method for the *in vivo* quantification of choline-containing compounds in breast tumors by proton MR spectroscopy at 1.5 Tesla. Magn Reson Med 2001;46:189–192. [PubMed: 11443726]
52. Cavassila S, Deval S, Huegen C, van Ormondt D, Graveron-Demilly D. Cramer-Rao bounds: an evaluation tool for quantitation. NMR Biomed 2001;14(4):278–283. [PubMed: 11410946]
53. Bolan, PJ.; Aufferman, WF.; Henry, PG.; Garwood, M. Feasibility of computer-intensive methods for estimating the variance of spectral fitting parameters. Proceedings of the 12th Annual Meeting ISMRM; Kyoto. 2004. p. 304
54. Ratiney, H.; Chung, S.; Henry, RG.; Srinivasan, R.; Nelson, SJ.; Pelletier, D. Bootstrap in MRSI: a non-parametric way to assess quantification standard error. Proceedings of the 15th Annual ISMRM; Berlin. 2007. p. 1402
55. Young K, Khetselius D, Soher BJ, Maudsley AA. Confidence images for MR spectroscopic imaging. Magn Reson Med 2000;44(4):537–545. [PubMed: 11025509]
56. Roebuck JR, Cecil KM, Schnall MD, Lenkinski RE. Human breast lesions: characterization with proton MR spectroscopy. Radiology 1998;209:269–275. [PubMed: 9769842]
57. Baik, HM.; Chen, JH.; Yu, H.; Mehta, R.; Nalcioglu, O.; Su, MY. Quantitative MR spectroscopy to monitor treatment response of breast cancer to neoadjuvant chemotherapy. Proceedings of the 15th Annual ISMRM; Berlin. 2007. p. 556
58. Graham SJ, Stanchev PL, Lloyd-Smith JO, Bronskill MJ, Plewes DB. Changes in fibroglandular volume and water content of breast tissue during the menstrual cycle observed by MR imaging at 1.5 T. J Magn Reson Imaging 1995;5(6):695–701. [PubMed: 8748488]
59. Manton DJ, Chaturvedi A, Hubbard A, Lind MJ, Lowry M, Maraveyas A, Pickles MD, Tozer DJ, Turnbull LW. Neoadjuvant chemotherapy in breast cancer: early response prediction with quantitative MR imaging and spectroscopy. Br J Cancer 2006;94 (3):427–435. [PubMed: 16465174]

60. Sijens PE. Human breast cancer *in vivo*: H-1 and P-31 mr spectroscopy at 1.5 T. Radiology 1988;169:615–620. [PubMed: 2847230]
61. Jagannathan NR, Singh M, Govindaraju V, Raghunathan P, Coshic O, Julka PK, Rath GK. Volume localized *in vivo* proton MR spectroscopy of breast carcinoma: variation of water-fat ratio in patients receiving chemotherapy. NMR Biomed 1998;11(8):414–422. [PubMed: 10221584]
62. Thomas MA, Binesh N, Yue K, DeBruhl N. Volume-localized two-dimensional correlated magnetic resonance spectroscopy of human breast cancer. J Magn Reson Imaging 2001;14(2):181–186. [PubMed: 11477678]
63. Gribbestad IS, Singstad TE, Nilsen G, Fjosne HE, Engan T, Haugen OA, Rinck PA. *In vivo*^{1}H MRS of normal breast and breast tumors using a dedicated double breast coil. J Magn Reson Imaging 1998;8(6):1191–1197. [PubMed: 9848727]
64. McIntosh, AD.; Corum, C.; Bolan, PJ.; Styczynski, A.; Powell, N.; Everson, LI. A Quantitative analysis of water T2 measurements in benign and malignant breast lesions *in vivo* at 4 Tesla. Proceedings of the 92nd Annual Meeting RSNA; Chicago. 2006.
65. Jacobs MA, Ouwerkerk R, Wolff AC, Stearns V, Bottomley PA, Barker PB, Argani P, Khouri N, Davidson NE, Bhujwalla ZM, Bluemke DA. Multiparametric and multinuclear magnetic resonance imaging of human breast cancer: current applications. Technol Cancer Res Treat 2004;3(6):543–550. [PubMed: 15560711]
66. Mountford CE, Somorjai RL, Malycha P, Gluch L, Lean C, Russell P, Barraclough B, Gillett D, Himmelreich U, Dolenko B, Nikulin AE, Smith IC. Diagnosis and prognosis of breast cancer by magnetic resonance spectroscopy of fine-needle aspirates analysed using a statistical classification strategy. Br J Surg 2001;88(9):1234–1240. [PubMed: 11531873]
67. Sijens, PEJadBM.; Nowak, PJ.; van Dijk, P.; Oudkerk, M. ^{1}H chemical shift imaging reveals loss of brain tumor choline signal after administration of Gd-contrast. Magn Reson Med 1997;37(2):222–225. [PubMed: 9001146]
68. Taylor, JS.; Reddick, WE.; Kingsley, PB.; Ogg, RJ. Proton MRS after gadolinium contrast agent. Proceedings of the 3rd Annual Meeting ISMRM; Nice, France. 1995. p. 1854
69. Lin, A.; Ross, BD. The effect of gadolinium on quantitative short-echo time single voxel MRS of treated and untreated brain tumors. Proceedings of the 8th Annual Meeting ISMRM; Denver, USA. 2000. p. 390
70. Smith JK, Kwock L, Castillo M. Effects of contrast material on single-volume proton MR spectroscopy. AJNR Am J Neuroradiol 2000;21(6):1084–1089. [PubMed: 10871019]
71. Bolan, PJ.; Baker, E.; DelaBarre, L.; Merkle, H.; Yee, D.; Everson, LI.; Garwood, M. Effects of Gd-DTPA on breast ^{1}H MRS at 4T. Proceedings of the 87th Annual Meeting RSNA; Chicago. 2001. p. 65
72. Joe BN, Chen VY, Salibi N, Fuangtharntip P, Hildebolt CF, Bae KT. Evaluation of ^{1}H-magnetic resonance spectroscopy of breast cancer pre- and postgadolinium administration. Invest Radiol 2005;40(7):405–411. [PubMed: 15973131]
73. Jagannathan NR, Kumar M, Seenu V, Coshic O, Dwivedi SN, Julka PK, Srivastava A, Rath GK. Evaluation of total choline from *invivo* volume localized proton MR spectroscopy and its response to neoadjuvant chemotherapy in locally advanced breast cancer. Br J Cancer 2001;84(8):1016–1022. [PubMed: 11308247]
74. Cecil KM, Schnall MD, Siegelman ES, Lenkinski RE. The evaluation of human breast lesions with magnetic resonance imaging and proton magnetic resonance spectroscopy. Breast Cancer Res Treat 2001;68(1):45–54. [PubMed: 11678308]
75. Kim JK, Park SH, Lee HM, Lee YH, Sung NK, Chung DS, Kim OD. *In vivo*^{1}H-MRS evaluation of malignant and benign breast diseases. Breast 2003;12(3):179–182. [PubMed: 14659324]
76. Huang W, Fisher PR, Dulaimy K, Tudorica LA, O'Hea B, Button TM. Detection of breast malignancy: diagnostic MR protocol for improved specificity. Radiology 2004;232(2):585–591. [PubMed: 15205478]
77. Bartella, L.; Thakur, S.; Morris, EA.; Liberman, L.; Huang, W.; Dershaw, DD. Proton magnetic resonance spectroscopy of the breast: does normal breast parenchyma give a false positive choline peak?. Proceedings of the 92nd Annual Meeting RSNA; Chicago. 2006. p. 178

78. Katz-Brull R, Lavin PT, Lenkinski RE. Clinical utility of proton magnetic resonance spectroscopy in characterizing breast lesions. J Natl Cancer Inst 2002;94(16):1197–1203. [PubMed: 12189222]

79. Jacobs MA, Barker PB, Argani P, Ouwerkerk R, Bhujwalla ZM, Bluemke DA. Combined dynamic contrast enhanced breast MR and proton spectroscopic imaging: a feasibility study. J Magn Reson Imaging 2005;21(1):23–28. [PubMed: 15611934]

80. McIntosh, AD.; Bolan, PJ.; Meisamy, S.; Corum, CA.; Styczynski, A.; Everson, LI. Evaluation of 118 women with radiographic breast abnormalities using high field quantitative ^{1}H MRS and DCE MRI *in vivo*. Proceedings of the 91st Annual Meeting RSNA; Chicago. 2005. p. 178

81. Baik, HM.; Yu, H.; Chen, JH.; Nalcioglu, O.; Su, MY. Correlation between choline and contrast enhancement in human breast cancer measured by quantitative ^{1}H single-voxel MR spectroscopy and dynamic contrast-enhanced MRI. Proceedings of the 15th Annual ISMRM; Berlin. 2007. p. 2803

82. Merkle, H.; DelaBarre, L.; Bolan, PJ.; Baker, EH.; Everson, LI.; Yee, D.; Garwood, M. Transceive quadrature breast coils and applications at 4 Tesla. Proceedings of the 9th Annual Meeting ISMRM; Glasgow. 2001. p. 1114

83. Danishad, KA.; Seenu, V.; Jagannathan, NR. 2D MRSI in locally advanced breast cancer: assessment of tumor response in patients undergoing neo-adjuvant chemotherapy. Proceedings of the 15th Annual ISMRM; Berlin. 2007. p. 557

84. Tkac, I.; Oz, G.; Gruetter, R. Comparison of metabolite quantification in the human brain at 4 and 7 Tesla. Proceedings of the 13th Annual ISMRM; Miami. 2005. p. 2458

85. Bartella L, Morris EA, Dershaw DD, Liberman L, Thakur SB, Moskowitz C, Guido J, Huang W. Proton MR spectroscopy with choline peak as malignancy marker improves positive predictive value for breast cancer diagnosis: Preliminary study. Radiology 2006;239(3):686–692. [PubMed: 16603660]

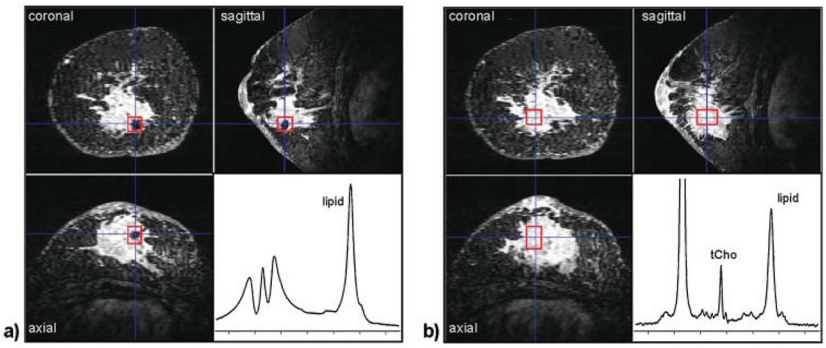

Figure 1.

Effect of radiographic markers on shim quality. Both (a) and (b) show a three-view multi-planar reconstruction of a 3D, fat-suppressed, post-contrast image acquired at 4 T in a patient with an invasive ductal carcinoma. The voxel ROI (red box) in (a) is placed directly over a metallic radiographic marker. Even after manual adjustment of the linear B_0 shims, the spectral quality is very poor. In (b) the voxel ROI was repositioned in the center of the lesion away from the marker, and a high-quality spectrum showing tCho and other metabolites could be obtained.

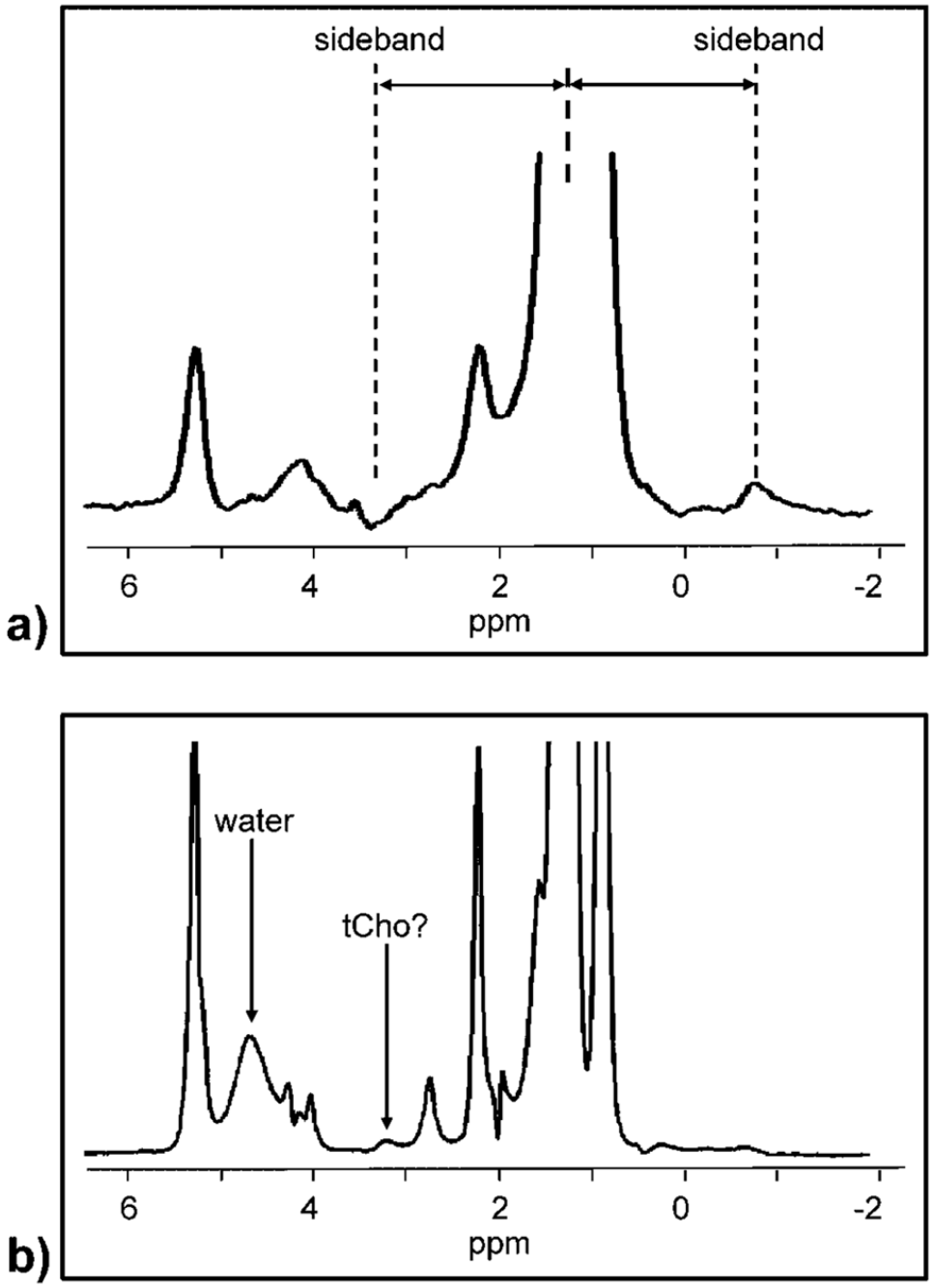

Figure 2.

Demonstration of two problems associated with lipid resonances. The spectrum in (a) is a water-suppressed, single-*TE* acquisition from a single voxel placed in a suspicious lesion. The large lipid resonance produces sideband artifacts on either side of the large lipid resonance, in-phase with the spectrum at ~−0.9 ppm and out-of-phase at 3.2 ppm. Depending on their phase, such sidebands can mimic or obscure a true tCho resonance. Lipid suppression or *TE* averaging can suppress these artifacts (14). The spectrum in (b) is a *TE*-averaged spectrum acquired without water or lipid suppression from a voxel placed intentionally in normal adipose tissue. Sidebands here are mostly suppressed but there is still a coherent resonance at ~3.2 ppm. This is not a sideband, as it does not have an anti-phase peak at − 1.9 ppm; rather it is probably a

trimethylamine moiety from the adipose lipids. Fitting and quantifying this resonance using water as an internal reference leads to [tCho] = 52.3 ± 11 mmol/kg, which is not physiologically reasonable and indicates that the 3.2 ppm signal does not originate from a water-soluble molecule.

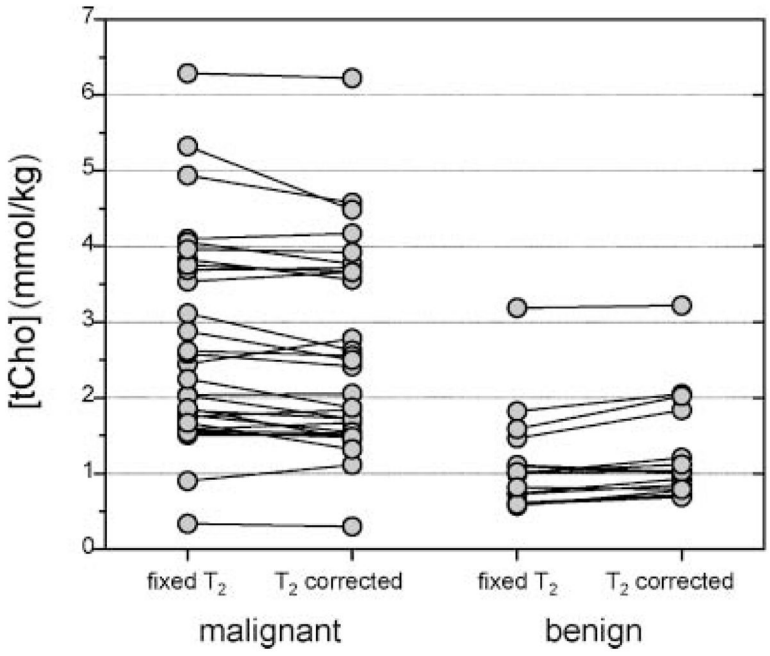

Figure 3.

Effect of water T_2 on relaxation corrections for quantitative MRS. The malignant lesions have a shorter water T_2 value (n = 29, T_2 = 56.7 ± 8.9 ms) than the benign lesions (n = 15, T_2 = 75.6 ± 17.3 ms). The tCho concentrations calculated using a fixed water T_2 value (60 ms) and the individually measured water T_2 values are compared for the two groups. On average, the use of individual T_2 corrections decreased the [tCho] in malignant lesions (from 2.75 ± 1.39 to 2.61 ± 1.33 mmol/kg) and increased the [tCho] in benign lesions (from 1.16 ± 0.67 to 1.29 ± 0.70 mmol/kg), thus reducing the difference between these groups. Without correction, the p-value for a one-sided *t*-test for the difference between benign and malignant is 0.00007; after correction the difference is smaller, with a p-value of 0.0004.

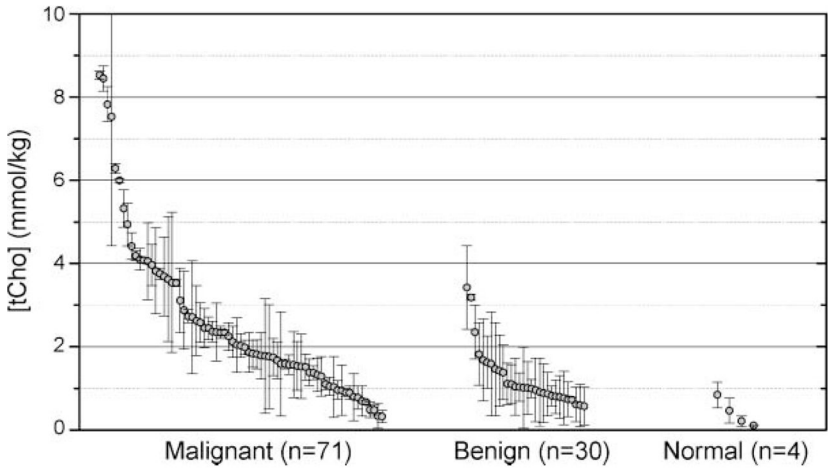

Figure 4.

Update of all biopsy-confirmed quantitative [tCho] measurements made at 4 T with non-zero values. Each measurement shows the calculated [tCho] value and Cramér–Rao error. This compilation includes data from several study protocols, but including only those measurements made before any radiation or chemotherapy treatments. This is an updated version of Fig. 6 from ref. (15). Comparing only the benign and malignant measurements, an ROC analysis leads to a cutoff of 1.45 mmol/kg, giving 73.2% sensitivity and 76.7% specificity for distinguishing benign from malignant lesions.

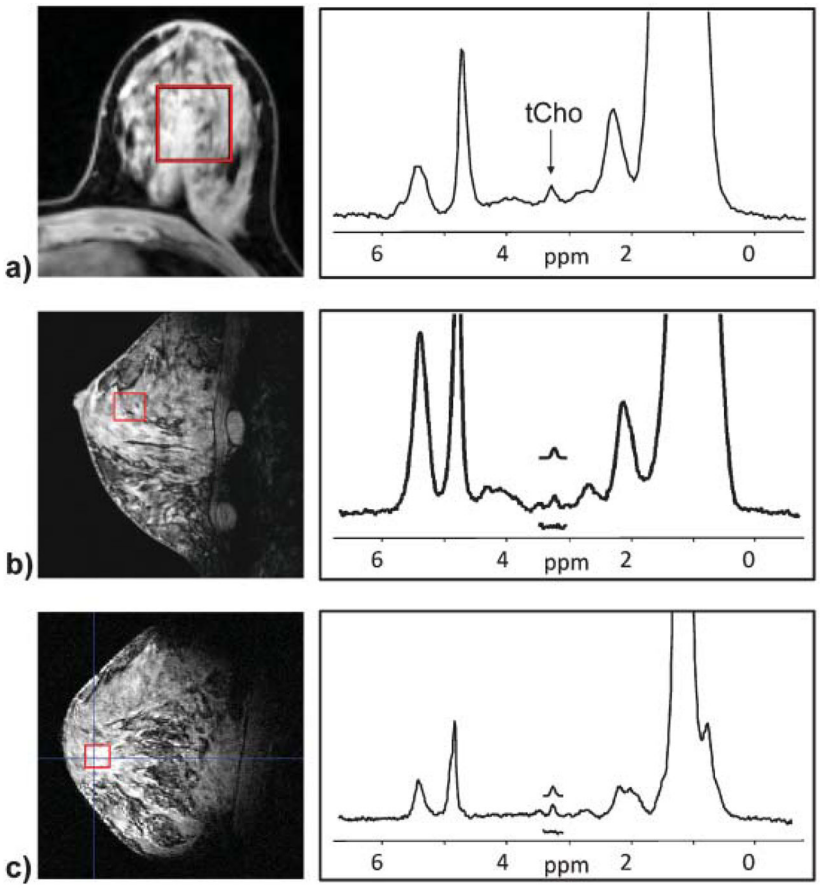

Figure 5.
Examples of detectable tCho resonances in normal subjects at high B_0 fields. Spectra were acquired in fibroglandular tissue in healthy subjects with no history of breast disease at (a) 3 T, (b) 4 T, and (c) 7 T.

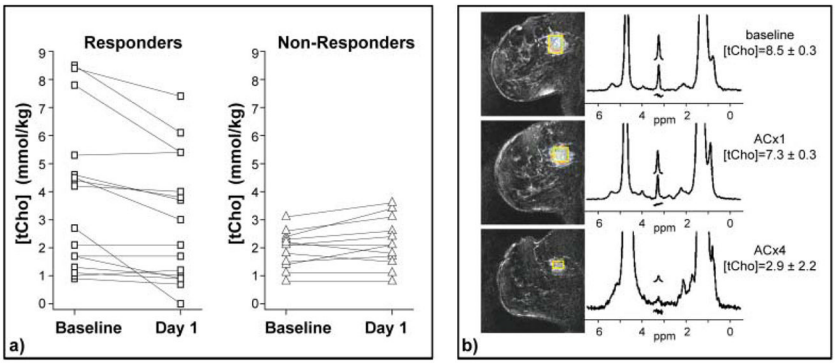

Figure 6.

Monitoring response to treatment with 4 T quantitative breast MRS. This is an update of findings previously reported in Meisamy *et al*. (17). These data include 28 patients measured with 4 T breast MRI/MRS before the start of chemotherapy, 1 day after the first dose of therapy, and after the complete course of treatment. The [tCho] measurements are shown for the baseline and day-1 measurements in (a): 75% of the objective responders showed a decrease in [tCho] at day 1 after therapy, whereas 92% of non-responders showed no change or an increase at the same time point. (b) An example of an objective responder, showing decreased [tCho] at day 1, and a clear anatomical response by the end of therapy (ACx4).

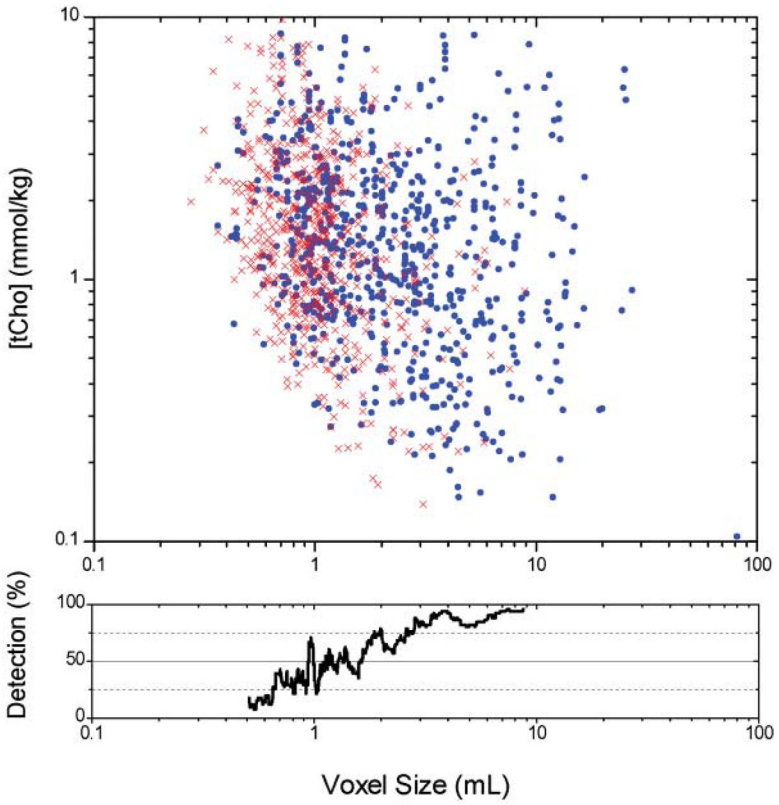

Figure 7.

Limits of tCho detection at 4 T. The top chart shows the relationship between [tCho] concentration and voxel size for a total of 1359 *in vivo* breast spectra acquired at 4 T including benign, malignant, and healthy tissues, acquired with 64–256 averages. Blue circles (735 spectra) indicate spectra in which a tCho resonance met the detection criteria (Cramér–Rao bound ≤ 100%); the red 'X' (624 spectra) indicate estimated errors for spectra in which the tCho resonance was not detectable. The range of detectable tCho resonances was 0.08–8.6 mmol/kg, with a median value of 1.4 mmol/kg. The lower plot shows the percentage of spectra with detectable tCho as a function of voxel size; voxels larger than 2.5 mL had a detectable tCho >75% of the time. These plots show that [tCho] is independent of voxel size, but the detectability of tCho increases with larger voxels.

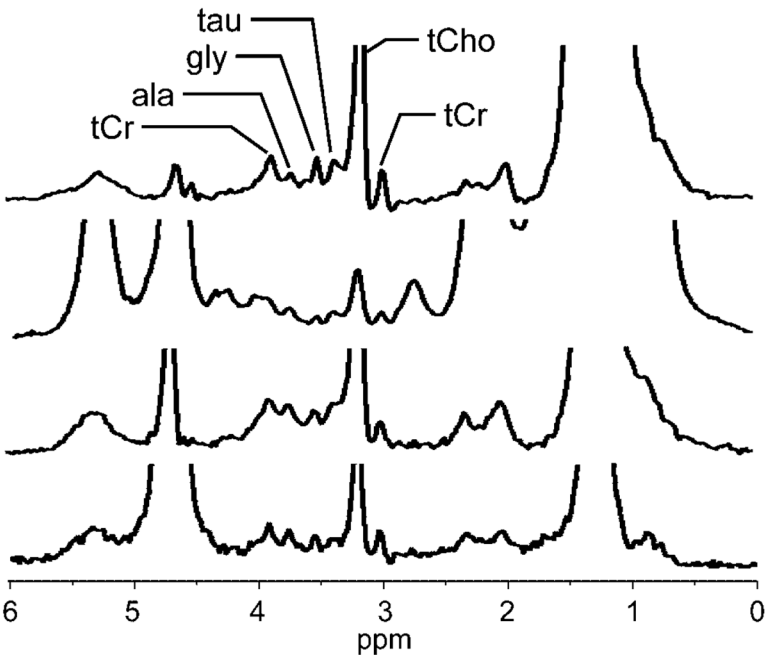

Figure 8.

Examples of high-quality 4 T breast spectra showing additional metabolites. These spectra all show a clear tCho resonance as well as several resonances previously reported only in *ex vivo* studies. Considering chemical shift and relative signal amplitudes, and using the *ex vivo* magic-angle spinning data from Sitter *et al*. (3) as a reference, resonances were identified as tCr = total creatine CH_3 (3.03 ppm) and CH_2 (3.92 ppm), tCho = total choline-containing compounds (3.22 ppm), tau = taurine (3.42 ppm), gly = glycine (3.55 ppm), ala = alanine (3.78 ppm).

Table 1

In vivo

MRS measurements of relaxation times in breast

	1.5 T		4 T		7 T	
	T_1	T_2	T_1	T_2	T_1	T_2
Water	440 ± 69[d†] 746 ± 118[e]	97 ± 10[e] 75 ± 20[d] 47–130[f]	870 ± 325[b†] 1860 ± 324[c]	60 ± 7[b]	2265 ± 65[c]	35.5 ± 5[c]
Lipid (1.3 ppm)	—	—	480 ± 100[b]	69 ± 12[b]	482 ± 13[c]	74 ± 7[c]
tCho	1513 ± 156[e] 1210[d]	320, 360[a] 269 ± 61[e] 181 ± 46[d]	—	399 ± 133[b]	—	—

[a] Bakken *et al.* (51).

[b] Bolan *et al*. (15).

[c] Bolan *et al*. (21).

[d] Tan *et al.* (48).

[e] Baik *et al*. (40).

[f] Manton *et al*. (59).

† T_1 measurements made after contrast.